proceedings

MDPI

Proceedings

Defect Detection in GFRP Plates Using Electromagnetic Induction Testing Using Autoencoder †

Wataru Matsunaga [1]*, Yoshihiro Mizutani [2] and Akira Todoroki [3]

[1] School of Engineering, Department of Mechanical Engineering, Tokyo Institute of Technology, Tokyo 152-8550, Japan
[2] School of Engineering, Department of Mechanical Engineering, Tokyo Institute of Technology, Tokyo 152-8550; ymizutan@mes.titech.ac.jp
[3] School of Engineering, Department of Mechanical Engineering, Tokyo Institute of Technology, Tokyo 152-8550; todoroki.a.aa@m.titech.ac.jp
* Correspondence: wmatsuna@ginza.mes.titech.ac.jp; Tel.: +81-3-5734-3178
† Presented at 1st International Electronic Conference on Applied Sciences, 10–30 November 2020; Available online: https://asec2020.sciforum.net/.

Published: 10 November 2020

Abstract: Electromagnetic induction testing is effective non-destructive testing (NDT) method not only for electrical conductive materials but also for non-electrical conductive materials. In the previous our research, electromagnetic induction testing method by using the DFL (Driver Field Lens) was proposed to inspect cracks in non-electrical conductive materials. In this research, the applicability of the autoencoder to the data processing for the data measured by the proposed method was examined. In particular, it was examined to separate the data on the specimen with the crack in the particular orientation (severe crack) from the data with both the other orientation (non-severe crack) or the without cracks. It was found that severe crack data and others cannot be divided into two simply by determining a threshold. However, the autoencoder can be utilized for the first screening of the obtained data to separate non-severe crack or without crack data from the data which include the severe crack data (non-severe crack, severe crack and without crack data). In general, the number of non-severe crack or without crack-data is often large compared to the number of severe crack-data. Therefore, the proposed first screening method using autoencoder can be useful when conducting the inspection by the electromagnetic induction testing method with the DFL.

Keywords: Autoencoder; Electromagnetic induction testing; GFRP

1. Introduction

Eddy current testing (ECT) is widely used for the inspection of electrical conductive materials in engineering field. For example, ECT is used for the inspection of heat transfer pipes of heat exchangers [1]. In general, ECT uses kHz range AC current to inspect high-electrical conductive materials, although, a few MHz AC current is used when low-electrical conductive materials, such as carbon fiber reinforced plastics, are inspected [2]. Furthermore, ECT becomes applicable to even non-electrical conductive materials by using much higher frequency. When the inspection target is non-electrical conductive materials, displacement current becomes the key parameter to detect a crack instead of eddy current and the NDT method is called as electromagnetic induction testing instead of ECT.

Previous researches showed the effectiveness for electromagnetic induction testing to inspect non-electrical conductive materials. Mizukami et al. reported that the method was able to detect the

crack and local thinning in GFRP [3]. Gäbler et al. showed the method was able to detect poor curing for resin [4].

The severity of cracks changes depending on the relationship between the orientation of the crack and the direction of the principal stress. Though, in the previous our research, we proposed the new method to use rotating DFL （Driver Field Lens）during the inspection to determine crack orientation to separate severe cracks from non-severe cracks.

The details of the method will be explained in the next chapter, but the output of the pickup coil changes depending on the relationship between the DFL angle and the crack orientation. However, high skill is required to judge the presence of cracks and estimate the orientation of the crack from output of pickup coil as the output changes in complicated manner with the DFL angle.

An autoencoder, one of the unsupervised learning methods in artificial neural network (ANN), is said to be used for anomaly detection [5]. In this study, the applicability of an autoencoder to solve above problem is examined.

2. Methods

2.1. Training data and evaluation data

Experimental setup is shown in Fig. 1. Training data and evaluation data were prepared by using this setup. This experimental setup is the same as the setup used in the previous research which demonstrated the effectiveness to evaluate permittivity [3]. In this research, sound GFRP plates and GFRP plates with cracks of various widths (1, 3 and 5 mm) and length (5, 10, 15 and 25 mm) were prepared. The Driver coil and the pickup coil were set above the specimen. Lift-off (distance between specimen surface and coils) of both coils was controlled to 1.5 mm. The 1.0 mm thick DFL was inserted between specimen and the coils. The DFL is rectangular coil made of copper tape which length and width are 60 mm and 15 mm respectively. The DFL is used to confine the magnetic field generated by the driver coil, and to control the magnetic field around the inspection area. Function generator (NI-PXI-5421, National Instruments) was connected to the driver coil and AC voltage with a maximum voltage of 100 mV and a frequency of 6 MHz was applied to the driver coil which was set above the specimen. Displacement current was induced by the driver coil and the change of the magnetic field was measured by the pickup coil and digitized by A/D converter (PicoScope 5244A, Pico Technology). The converter was connected to PC and the obtained data was analyzed by the software (LabVIEW 2018, National Instruments). As shown in Fig. 1 (a), origin of coordinates was defined at the center of the specimen. The driver coil, pickup coil and DFL were scanned along x-axis while keeping them at the same distance from x = −53 mm to x = 47 mm. At each position, the DFL was rotated from 0 to 180 degrees with 15 degrees step. The definition of the DFL angle is shown in Fig. 1 (b). By rotating the rectangular DFL, the displacement current field changes depending on the relationship between the direction of the DFL and the direction of the crack.

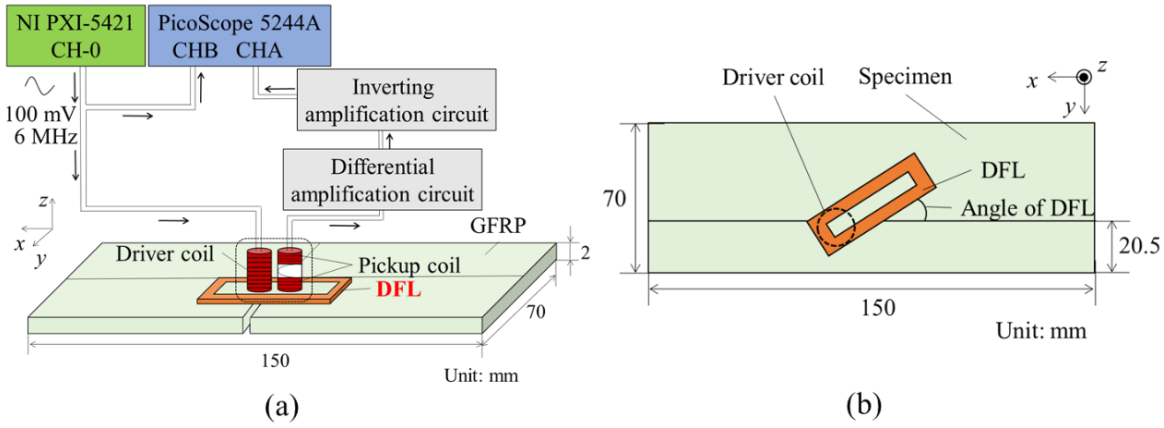

Figure 1. Schematic of experimental setup. (**a**) Over view of the experimental setup; (**b**) the definition of angle and position for the DFL.

At every DFL angle at each x-position, the both the input data to the driver coil and the output data from the pickup coil were measured 30 times, and the average values were recorded separately as the measured values at that DFL angle of that x-position. By scanning the coil pair from x = −53 mm to 47 mm, 23 × 2 data were obtained for each DFL angle for each specimen. In this study, the output data when the DFL angle matches with the crack angle is used as normal data for the autoencoder. Since the crack orientations of the cracked GFRP plates used in this study are all 90 degrees, the data when the DFL is 90 degrees is used as the normal data and used for training the autoencoder. Table 1 shows specifications of the specimens used for acquiring normal data for the autoencoder. Table 2 and 3 show specifications of the specimens used for acquiring anomaly data. The normal data and the anomaly data were combined and used as evaluation data for the autoencoder. The training data should not be included for the evaluation data if an accurate analysis is to be performed, but due to the small number of the data, we decided to use it this time.

Table 1. Specifications of the specimens used for acquiring normal data for the autoencoder.

Crack length [mm]	Crack width [mm]	DFL angle [°]
20	3	90
45	3	90
35	2	90
35	6	90
20	2	90
20	6	90
45	2	90
45	6	90
35	1	90
35	3	90
35	5	90
5	1	90
10	1	90
15	1	90
25	1	90
0	0	90

Table 2. Specifications of the specimens used for acquiring anomly data.

Crack length [mm]	Crack width [mm]	DFL angle [°]
20	3	60, 210
45	3	60, 80, 210
35	2	60, 80, 210
35	6	60, 80, 210
35	3	80, 110, 210, 270
20	6	80, 210
45	2	80, 210
45	6	80, 210

Table 3. Specifications of the specimens used for acquiring anomly data.

Crack length [mm]	Crack width [mm]	DFL angle [°]
35	1	0, 15, 30, 45, 60, 75, 105, 120, 135, 150, 165, 180
35	3	0, 15, 30, 45, 60, 75, 105, 120, 135, 150, 165, 180
35	5	0, 15, 30, 45, 60, 75, 105, 120, 135, 150, 165, 180
5	1	0, 15, 30, 45, 60, 75, 105, 120, 135, 150, 165, 180
10	1	0, 15, 30, 45, 60, 75, 105, 120, 135, 150, 165, 180
15	1	0, 15, 30, 45, 60, 75, 105, 120, 135, 150, 165, 180
25	1	0, 15, 30, 45, 60, 75, 105, 120, 135, 150, 165, 180
0	0	0, 15, 30, 45, 60, 75, 105, 120, 135, 150, 165, 180

2.2. Autoencoder

Figure 2 shows structure of the autoencoder used in this study. The programming was performed by using graphical neural network application (Neural Network Console, SONY). The upper module in the figure is the autoencoder and the bottom is module for calculating RMS error between input data and decoded data. In this autoencoder, the number of max epoch and bath size was set 1000 and 10 respectively.

At the upper module in Fig. 2, Input data (23 × 2) was compressed to 40 at the Affin layer and activated by the Tanh layer. The output from Tanh layer was dimensionally reduction data of input data. Then, these data were decoded by Affin layer and Tanh layer. The SquaredError layer was the loss function. During the training of the autoencoder, the weights in the ANN are optimized as the loss (the mean squared error between output data and decoded data) becomes minimize. Dropout layer was set after the input layer to improve the efficiency and accuracy for the training.

At the bottom module in Fig. 2, difference between Input data and decoded data were calculated at Sub2 layer. Root mean squared errors of the difference were calculated by PowScalar and Mean layers (23 × 2 ⇒ 1 × 2) and the mean for the errors was calculated at the Mean layer (1 × 2 ⇒ 1). Mulscaler layer was added at the end to disable the loss function (SquaredError). This is just an NNC's specific expression and will not be explained in detail here.

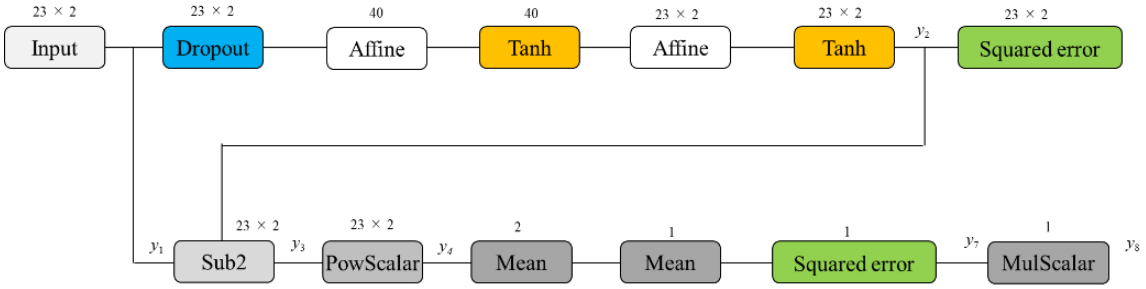

Figure 2. Schematic of the constructed autoencoder. The upper module is autoencoder and the bottom module is for calculating the difference between input data and decoded data.

3. Results and discussion

Both the normal data and the anomaly data explained in 2. 1 are put into the trained autoencoder. The root mean squared error between input data and decoded data (output from the autoencoder) was calculated. The histogram of the errors is shown in Fig. 3. The horizontal axis shows the error and the vertical axis shows the frequency of each error. The error in Fig. 3 are multiplied by 1000 as the original errors are quite small. The blue bar shows the frequency for the normal data when the angles of the DFL matches to that of crack. The red shows for the anomaly data when the angle does not match to the angle of a crack or when the crack does not exist.

As shown in the figure, the average error for the normal data is small, while the error for the anomaly data is large. As the error for the anomaly data is widely distributed and the error of some data is the same range as those for the normal data, normal data and anomaly data cannot be divided into two simply by determining a threshold. However, as average error and variation of the normal data are small, it is possible to separate the data not including normal data from the data including normal data by setting an appropriate threshold value. Though, the method can be utilized for the first screening of the obtained data to separate the data which took at the condition when the DFL angle is different from crack orientation (anomaly data: non-severe crack data + without crack data) from the data which include the data when the DFL angle is same as crack orientation (normal data + anomaly data: severe crack data + non-severe crack data + without crack data). In general, the number of non-severe crack-data or without crack-data is often large compared to the number of severe crack-data. Therefore, the first screening method by the proposed method using autoencoder can be useful when conducting the inspection by the electromagnetic induction testing method with the DFL.

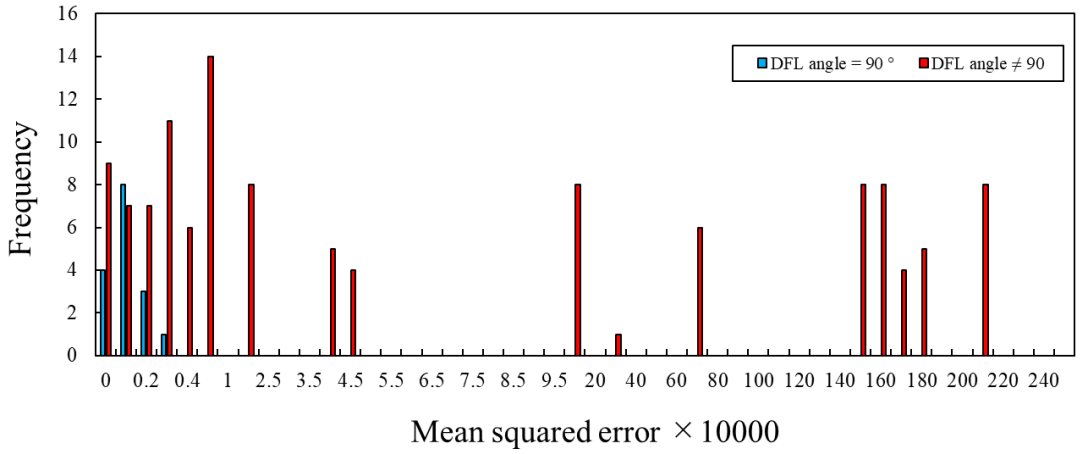

Figure 3. Histogram for mean squared value for the DFL angle = 90 degrees and the DFL angle ≠ 90 degrees.

4. Conclusions

In this research, the applicability of an autoencoder to separate the data for the crack with the particular orientation (severe crack) from those with other orientation (non-severe crack) and without cracks was examined. The data was obtained by using the electromagnetic induction testing with the DFL for GFRP specimens without cracks and with cracks of various widths, lengths and orientations.

It was found that severe crack data and the data for the non-severe crack and without crack cannot be divided into two simply by determining a threshold. However, the autoencoder can be utilized for the first screening of the obtained data to separate non-severe crack or without crack data from the data which include the severe crack data by determining an appropriate threshold.

References

1. Zhenmao Chena, Noritaka Yusa, Kenzo Miya. Enhancements of eddy current testing techniques for quantitative nondestructive testing of key structural components of nuclear power plants. *NUCL ENG DES* 2008, *Vol. 238*, pp. 1651-1656.
2. Martin H. Schulze, Henning Heuer, Martin Küttner, Norbert Meyendorf. High-resolution eddy current sensor system for quality assessment of carbon fiber materials. *Microsyst Technol* 2010, *Vol. 16* pp. 791-797.
3. Koichi Mizukami, Yoshihiro Mizutani, Akira Todoroki, Yoshiro Suzuki. Desigin of eddy current-based dielectric constant meter for defect detection in glass fiber reinforced plastics " *NDT&E Int* 2015, *Vol. 74*, pp. 24–32.
4. Simone Gäbler, Henning Heuer, Member, IEEE, Gert Heinrich. Measuring and Imaging Permittivity of Insulators Using High-Frequency Eddy-Current Devices, *IEEE Trans. Instrum Meas.* 2015, Vol. 64, pp. 2227-2238.
5. Jing Xie, Changhang Xu, Guoming Chen, Weiping Huang. Improving visibility of rear surface cracks during inductive thermography of metal plates using Autoencoder. *INFRARED PHYS TECHN* 2018, Vol. 91, pp. 233-242.